Numerical Modeling of Electron Cascade Processes Leading to Breakdown in Argon Gas

Dr. Bassam Ghazolin *

(Received 8 / 4 / 2022. Accepted 31 / 7 /2022)

□ ABSTRACT □

his research presents a general numerical modeling of electron cascade processes leading to breakdown in argon gas. The model succeed to interpret the breakdown phenomenon in argon gas over pressure range from $1.368x10^2$ torr to $2.35x10^3$ torr irradiated with the second harmonic of the Nd:galss laser of wave length is equal 0.53 μm and pulse duration is 15 ns. The output of the computer program enabled us to obtained some relations for the electron energy distribution function (EEDF) and its parameters.

The EEDF gradually decreases up 12 eV (first excitation limit) followed by a sharp decrease resulting in a tail at ε = 21 eV ending with a very small value of the EEDF ~1 to 10. This gradual decrease can be explained due to the fast energy gain in elastic processes associated with the laser filed which causes an accumulation of energy to values exceeding the excitation (or ionization) threshold of the gas atoms, eventually causing their excitation or ionization. This result clarifies that during the first half of the laser flash losses has no contribution to the values of the EEDF. The only parameter which affect these values is the laser intensity. At the end of the laser flash, however, a noticeable drop of the EEDF is observed when recombination losses are present.

Keywords: argon laser gaz - breakdown in argon gaz, Electron Energy Distribution Function (EEDF)

* **Associate Professor , Physics Section, Faculty of Science, Tishreen University, Lattakia, Syria.**
bassam.g@scs-net.org

النمذجة العددية لنموذج الالكترونات المتعاقبة التي تؤدي إلى انـهيار غاز الأرغون

د. بسام غزولين*

(تاريخ الإيداع 8 / 4 / 2022. قُبِل للنشر في 31 / 7 /2022)

□ ملخّص □

يقدم هذا البحث نمذجة عددية عامة لنموذج الالكترونات المتعاقبة التي تؤدي إلى انهيار غاز الأرغون. هذا النموذج يقدم تفسير لظاهرة انهيار غاز الارغون في مجال الضغط من torr $1.368x10^2$الى torr $2.35x10^3$ المشعع بجهاز Nd:galss ليزر توافقي بطول موجة 0.53□m و نبضة عرضها 15ns. مكنتنا مخرجات برنامج على الحاسب من دراسة تابع التوزيع لطاقة الالكترون (EEDF) ومتحولاته.

يتناقص تابع التوزيع لطاقة الالكترون EEDF تدريجيًا بمقدار 12 eV (حد الإثارة الأول) متبوعًا بانخفاض حاد عند النهاية ينتج عنه عند القيمة 21 eV =□□ ينتهي بقيمة صغيرة جدًا لقيمة هذا التابع EEDF بين 1 الى 10. يمكن تفسير هذا الانخفاض التدريجي بسبب اكتساب الطاقة السريع في العمليات المرنة المرتبطة بالليزر الذي يؤدي إلى تراكم الطاقة إلى قيم تتجاوز عتبة الإثارة (أو التأين) لذرات الغاز ، مما يؤدي في النهاية إلى الاثارة أو التأين. توضح هذه النتيجة أنه خلال النصف الأول نبضة الليزر لن تكون هنالك أي مساهمة للضياع على قيم التابع EEDF. الشيء الوحيد الذي يؤثر على هذه القيم هو فيمة شدة اشعاع الليزر. ومع ذلك، في نهاية نبضة الليزر، لوحظ انخفاض ملحوظ في قيم التابع EEDF عند وجود الضياع الناتج عن إعادة التوحيد ثلاثي الجسيمات.

الكلمات المفتاحية: انهيار ذرات الارغون في الليزر– توزع وانتشار طاقة الالكترونات في ذرات الأرغون، تابع التوزيع للطاقة للإلكترون EEDF

*استاذ مساعد، قسم الفيزياء ، كلية العلوم، جامعة تشرين، اللاذقية، سورية. bassam.g@scs-net.org

Introduction:

The generalized electron cascade model is mainly based on classical aspect of electron energy absorption from laser field.

In the present research, the model will be applied to argon gas. The interest of laser induced argon plasma is related to the interaction of laser radiation with metal targets during material processes (drilling, welding, etc…). In these case plasma plays an important role in energy conversion between laser and materials [1,2].

The plasma strongly absorbs and refracts the laser radiation and changes significantly the energy transfers from laser beam to the materials [3].

Before proceeding to describe the output of computational program, a brief description of the argon atom and the related coefficients for the various physical processes included into are given the following section.

Argon Atom:

In the case of argon atom, there are a large energy gap between their ground state and the first electronic excited state. This means that most of the excited states are lying at a very close distance to the ionization limit. The first excited state lies at about /11.5 eV/, while the ionization limit corresponds to /15.75 eV/. This means that all the electronic levels of this atom occupy an energy range of about 5 eV. Therefor taking the actual number of all these excitation levels into consideration dose not play an important role in the ionization mechanisms. In this research we adopt the idea [4] of considering the group of electronic excitation levels, lying above the first excited state, to be represented by the “4S” state (11.6 eV) . This metastable state is actually a composite of four lowest excited levels which are very closely spaced in energy (0.3eV) and the population of each are strongly mixed by electron collision. Consequently, treating these four states as a single state (for the purpose of calculating the contribution of the two-step ionization) is a good reasonable assumption and simplified the calculation [5].

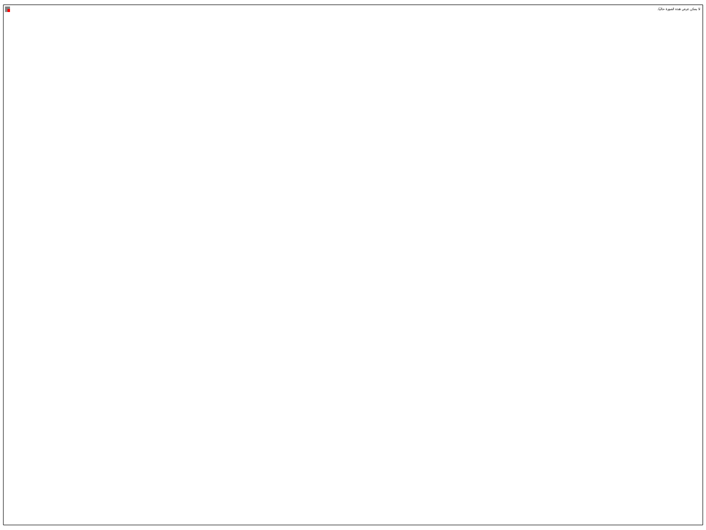

Figure (1) atomic structure of argon

We also considered the ,4p, excited state at (13.2 eV) as a representative state of all higher excited states, that lie in the range of ionization by collision with an electron; or by absorption of few photon (one or two) having the same amount of energy. Considering this atomic structure of argon shown in figure (1), The Growth Rate Of Electron

Concentrations Due to the Combined Action of Multiphoton and cascade Ionization Mechanisms [6,7,8,9,10]:

Electron Energy Distribution Function : The rate of change of the fraction of electrons f having energies between e and e+Δe . during the time interval Δt , due to the various possible interactions mentioned in the previous section is given by [4]:

$$\partial f/\partial t= G(\varepsilon)[(\partial f/\partial \varepsilon) +2\varepsilon (\partial^2 f/\partial \varepsilon^2)] +[B \{I(t)\}^k N(t) + \sum_L B_L\{I(t)\}^{kL} X_L(t)] +[\sum_L \nu_{xL}(\varepsilon+\varepsilon_{xL}) N(t) f(\varepsilon+\varepsilon_{xL}) + \nu_i(\varepsilon+\varepsilon_i) N(t) f(\varepsilon+\varepsilon_i)+ \sum_L \nu_{ixL} (\varepsilon +\varepsilon_i-\varepsilon_{xL})X_L(t) f(\varepsilon+\varepsilon_i-\varepsilon_{xL})] -[\sum_L \nu_{xL}(\varepsilon) N(t) f(\varepsilon) + \sum_L \nu_{ix}(\varepsilon) X_L(t) f(\varepsilon) + \nu_\iota(\varepsilon) N(t) f(\varepsilon)] + D(\varepsilon) \nabla^2 f(\varepsilon) - R(\varepsilon) n_+ (t) f(\varepsilon) f(\varepsilon) - r(\varepsilon) n_d(t) f(\varepsilon) \quad (1)$$

All The parameters involved in this equation are defined they will be defined, here. The first bracket on the right hand side of this equation represents the rate of electron energy gain from the laser field, and the parameters included are as described by equations (2) and (3). Therefore, the rate of the energy gain by free electrons from the laser field is represented by the equation [4]:

$$\partial f/\partial t =G(\varepsilon) [(\partial f / \partial \varepsilon) +2\varepsilon (\partial^2 f / \partial \varepsilon^2)] \quad (2)$$

Where, ε is the electron energy,

$$G(\varepsilon) =(1/ 3) \varepsilon_0 \nu_m$$
$$\varepsilon_0 = e^2 E^2 / 2 m \omega^2 = (377 e^2 /2 m \omega^2) I(t) \quad (3)$$

where ε_0 is the oscillatory energy of an electron of charge e and mass m , in laser with electric field amplitude E and angular frequency ω

$f=f(\varepsilon,t)$ is the electron density at any time t having energy between ε and ε+Δε

ν_m is the momentum transfer collision frequency between electrons and gas atoms.

The second bracket represents the rate of electrons generation due to ionization of atoms (from the ground state or any excited state (from the ground state or any excited state L) by multiphoton absorption processes. N(t) and XL(t) are the instantaneous density of atoms in their ground state and in any excited state L.

I(t) , the instantaneous laser intensity, is given by equations (2.16) and (2.21), and its exponent powers k and k_L are as defined in reactions equation (4) and (5), respectively.

$$A + k h\nu \longrightarrow A^+ + e \qquad k = < \varepsilon_i / h\nu > \quad (4)$$
$$A^{*L} + k_L h\nu \longrightarrow A^+ + e \qquad k_L =<(\varepsilon_i -\varepsilon_x)/h\nu> \quad (5)$$

where r and z are distances measured radially and axially from the focal spot, d is the spot diameter at the focal plane and L represents the distance between those points on either sides of the focal plane at which the intensity is half its maximum value I_o at the focal plane.

The third bracket is the rate of appearance of electrons in energy range ε to ε + Δε by the inelastic collisions (excitation and ionization collisions) with ground state atoms and ionization collisions with excited state atoms. Here $\nu_{xL}(\varepsilon)$, $\nu_\iota(\varepsilon)$ and $\nu_{ixL}(\varepsilon)$ are the collisional rate coefficients of electrons , in any energy range Δε, of excitation , ionization of neutral and excited atoms, respectively. The fourth bracket gives the loss rate of electrons, in the energy range ε to ε+ Δε , as a result of excitation and ionization collisions with ground state atoms as well as the ionization of the excited atoms. The last three terms are the loss rate of electrons in the energy range ε to ε+Δε due to diffusion , recombination n a three body reaction, and dissociative recombination process respectively. D, R and r are the coefficients of electron diffusion three body recombination and dissociative recombination. n_+ (t) and n_d (t) are the density of ions dimer ions at any time t.

Results and Discussions:

Results of Numerical Computations and Discussion:

The computer program was first run to investigate the variation of the breakdown threshold intensity of laser radiation as a function of the gas pressure. These calculations are performed under the experimental condition of Rosen and Weyl [7] for the second harmonic of Nd-glass laser of wavelength 0.53μm and pulse duration =15 ns irradiated argon gas over pressure range ($1.368x10^2$ - to $2.35x10^3$ torr).

Several calculations were done for varying values of the peak intensity at each gas pressure, and the total number produced at the end of laser flash was compared with breakdown criteria which in the experiment was assumed to be as a degree of the fractional ionization δ = 0.1% of the neutral gas atom present in the focal region.

The computed threshold intensity for breakdown was then obtained by interpolation between the calculated results. For each calculation a single initial electron of low energy was assumed to be present in the focal volume. To avoid these discontinuities in the distribution function f(ε) , this electron was represented as a Gaussian distribution of mean energy(4 eV) and standard deviation (2 eV) . The computer program listed the total number of electrons and excited atoms, for each considered energy state as well as a complete energy distribution for the free electrons which are created during the different intervals of laser flash. Figures (2,3,4,5) represent the variation of electron density at the end of laser flash as a function of laser peak intensity for each value of gas pressure. These curves enabled us to obtain the threshold intensities for breakdown as a function of gas pressure which satisfy the assumed breakdown criteria

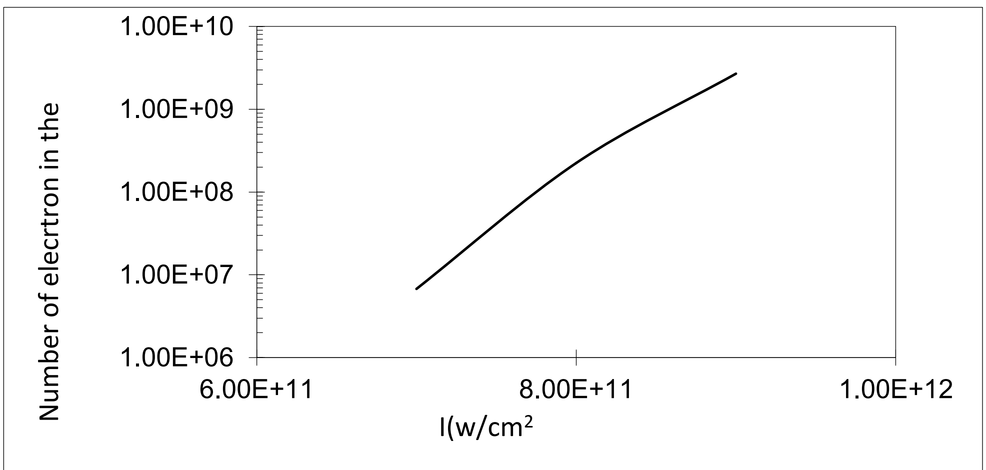

Figure (2) variation of electron density at end of 15 ns laser pulse length

($I = 0.53\ \mu m$) as a function of laser peak intensity at P=235.6 torr.

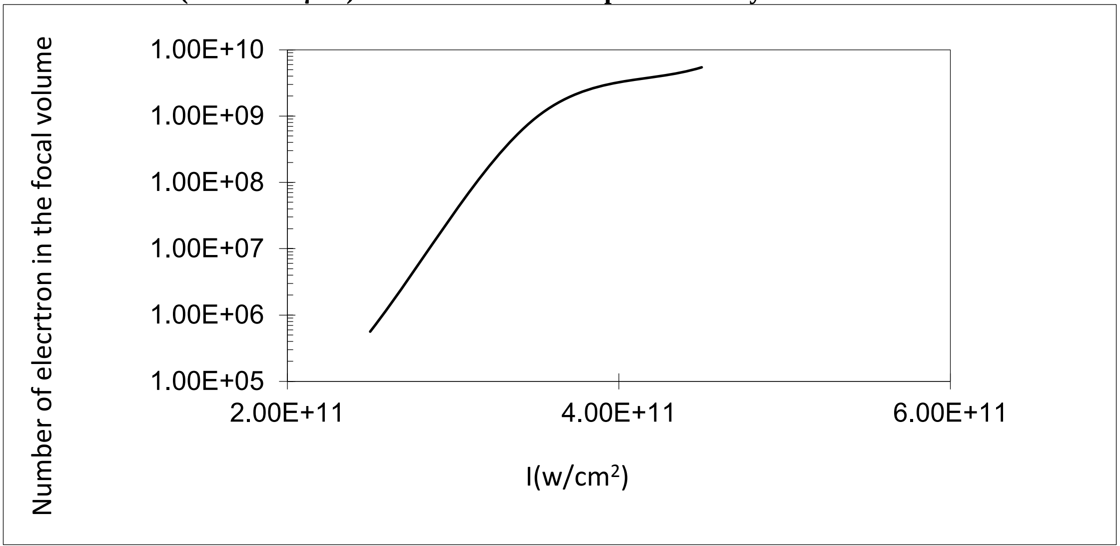

Figure (3) variation of electron density at end of 15 ns laser pulse length ($I = 0.53\ \mu m$) as a function of laser peak intensity at P=509.2 torr.

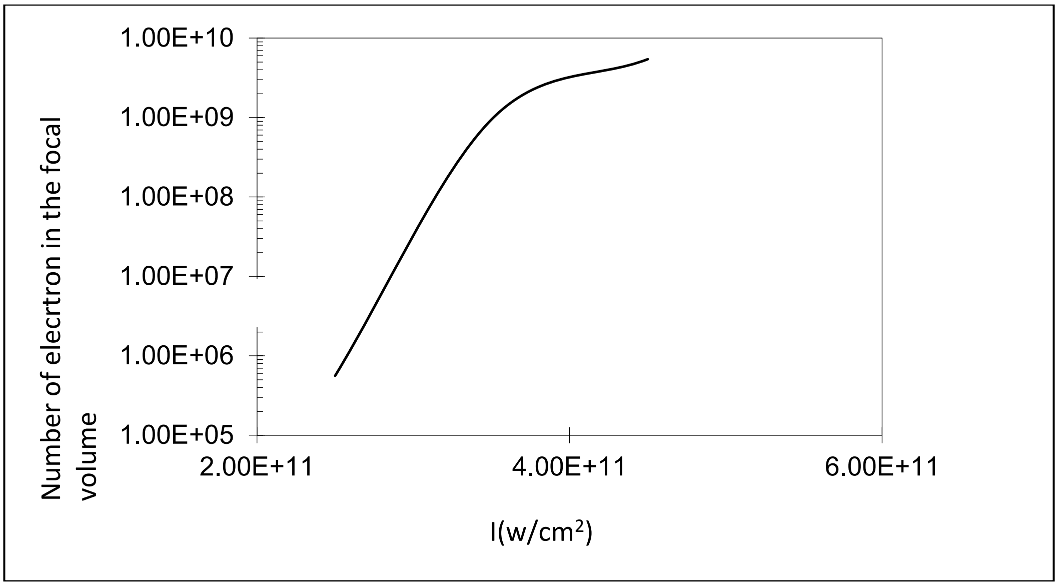

Figure (4) variation of electron density at end of 15 ns laser pulse length ($I = 0.53\ \mu m$) as a function of laser peak intensity at P=509.2 torr.

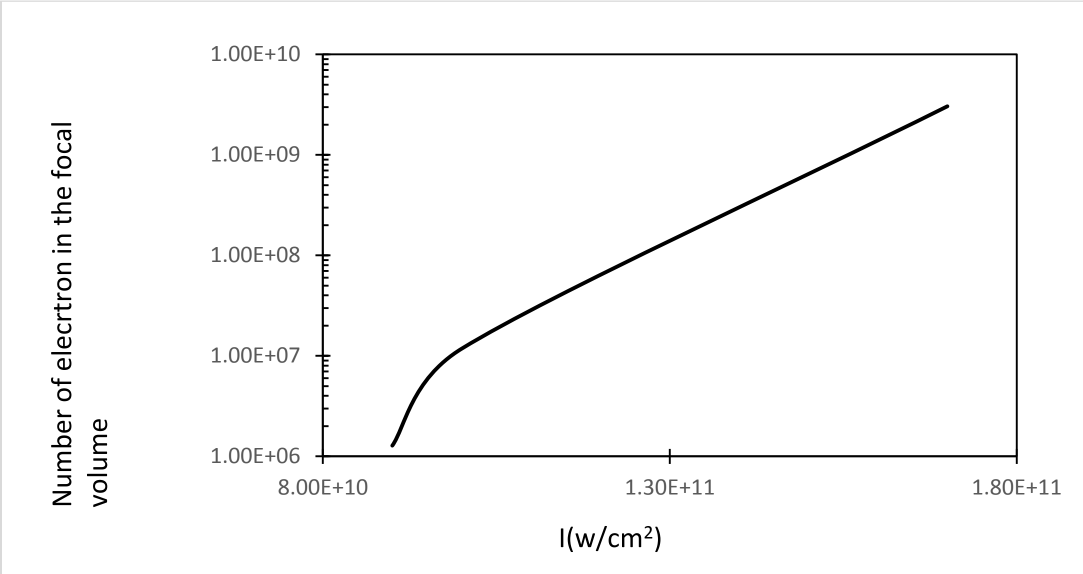

Figure (5) variation of electron density at end of 15 ns laser pulse length ($I = 0.53\ \mu m$) as a function of laser peak intensity at P=1520 torr.

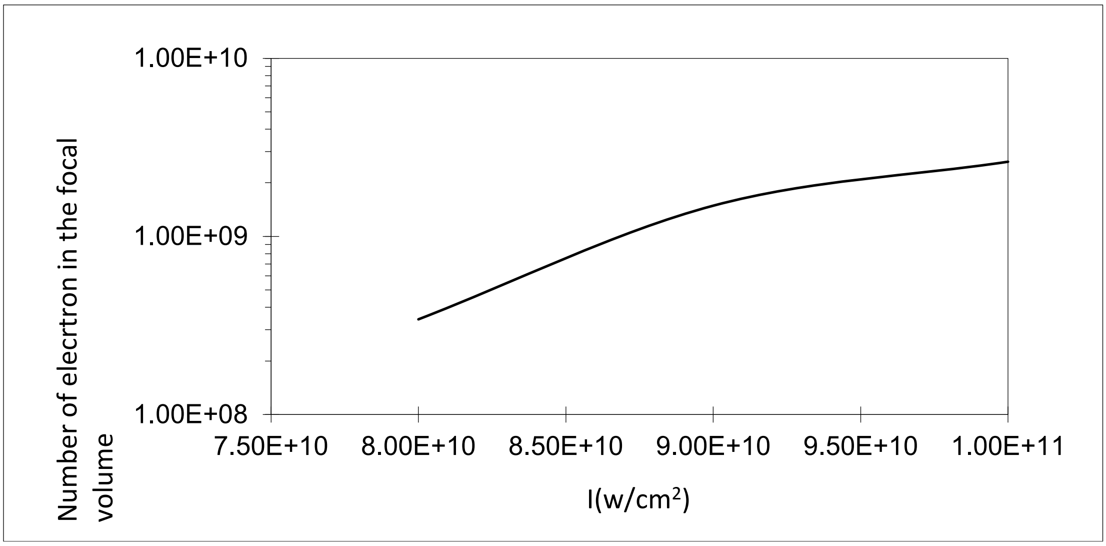

Figure (6) variation of electron density at end of 15 ns laser pulse length ($I = 0.53\ \mu m$) as a function of laser peak intensity at P=2350 torr.

The EEDF is calculated for case of gas pressure (P=2.356x10^2 torr) , with diffusion losses curve (I) at threshold intensity (I_{th}=8.6x10^{11} w/cm^2) , and with recombination losses at (I_{th}= 6.37x10^{11} w/cm^2) , for two different time interval of the laser flash (namely the peak and the end of the laser pulse) . Figures [7] and [8] illustrate the behavior of the EEDF at the peak and the end respectively.

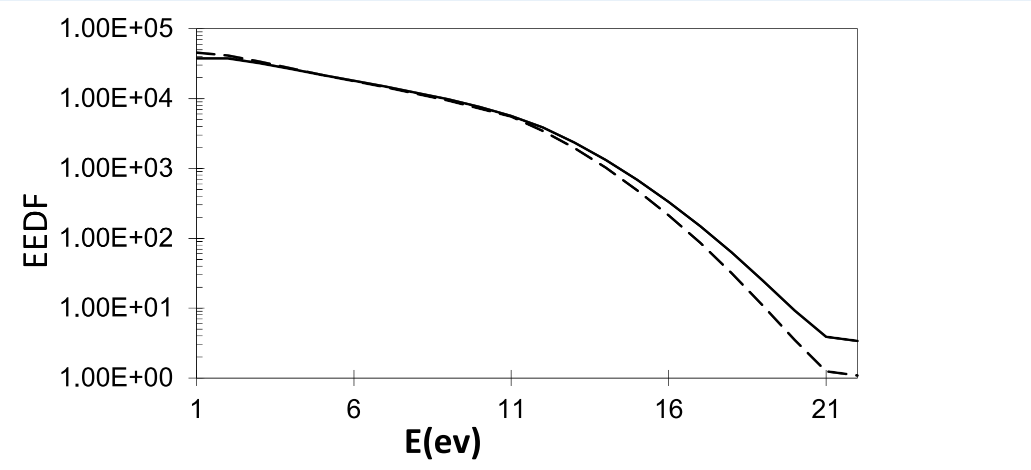

Figure (7) The EEDF at the peak of laser flash at P=2.356x10^2 torr, with I = 6.37x10^{11} w/cm^2 in the presence recombination loss (dashed line II), and with I = 8.6x10^{11} w/cm^2 in the presence of diffusion loss (solid line I).

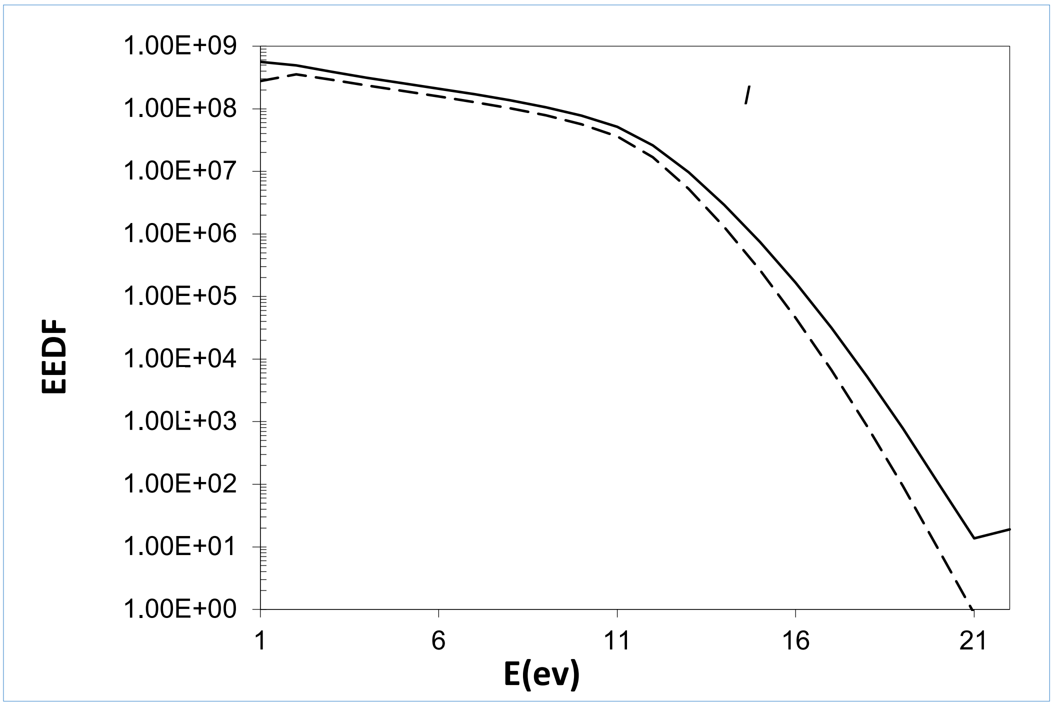

Figure (8) The EEDF at the end of laser flash at P=2.356x10^2 torr with I = 6.37x10^{11} w/cm^2 in the presence recombination loss (dashed line II), and with I = 8.6x10^{11} w/cm^2 in the presence of diffusion loss (solid line I)

It is clear from both figures (7 and 8) that the EEDF gradually decreases up 12 eV (first excitation limit) followed by a sharp decrease resulting in a tail at ε = 21 eV ending with a very small value of the EEDF ~1 to 10. This gradual decrease can be explained due to the fast energy gain in elastic processes associated with the laser filed which causes an accumulation of energy to values exceeding the excitation (or ionization) threshold of the gas atoms, eventually causing their excitation or ionization. This process results in a high population of low energy electrons which can repeat the same process very fast. As soon as the electrons gain enough energy, they can escape out of the focal volume, leading to the observed gradual decrease in the electron energy distribution function over this energy range. These electrons which can reach the excitation threshold (11.6 eV) they lose their energy and directed bake to feed the low energy region. It’s also noticed that over the energy range (2 - 11) eV the value of EEDF for the two curves (curves I and curve II) are coincidence , despite the difference of their laser intensity(I= $8.6\text{x}10^{11}$ w/cm^2 and I= $6.37\text{x}10^{11}$ w/cm^2). Beyond this energy rang curve (I) exceeds curve (II) up to their tails. the overall behavior of these curves can be attributed to fact that low energy electrons can escape from the focal volume causing a retardation in the growth of the low energy electrons and this in turn results lowing the values of the EEDF observed over the energy rang (2 to 11) eV , when electron diffusion is taken into account . Once electrons gain enough energy to undergo inelastic collision, their values increase due to the ionization and step wise ionization processes.

At the end of the laser flash figure (8) curve (I) exceeds curve (II) over the whole range of the electron energy. This behavior indicates that diffusion losses are not effective during the second half of the laser flash. The increase of the EEDF for curve (I) is due to the higher intensity considered for this curve.

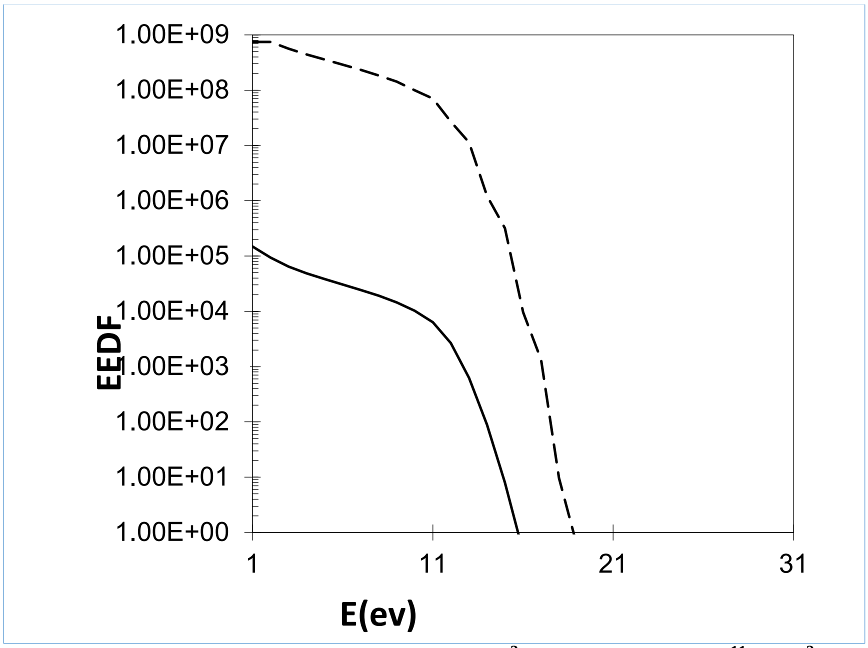

Figure [9] The EEDF at the peak of laser flash at P=$2.35\text{x}10^3$torr with I = $1.33\text{x}10^{11}$ w/cm^2 in the presence recombination loss (dashed line II), and with I = $9\text{x}10^{10}$ w/cm^2 in the presence of diffusion loss (solid line I).

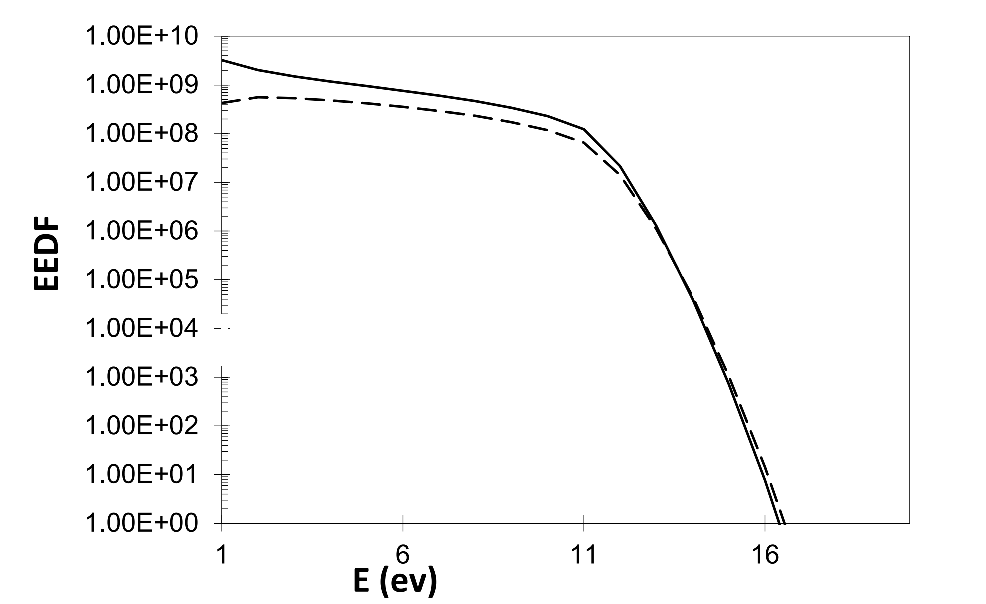

Figure [10] The EEDF at the peak of laser flash at P=2.35x10^3 torr with I = 1.33x10^{11} w/cm^2 in the presence recombination loss (dashed line II) , and with I = 9x10^{10} w/cm^2 in the presence of diffusion loss (solid line I) .

In figures [9] and [10] the same relation between the EEDF and the electron energy is plotted at high value of gas pressure (P=2.35x10^3 torr case 2), when diffusion losses are acting curve (I) and when recombination losses are dominating curve (II). It is shown from figure [8] that there is a quite difference between the two values of the EEDF for curve (I) and curve (II) over the whole range of the electron energy. This result clarifies that during the first half of the laser flash losses has no contribution to the values of the EEDF. The only parameter which affect these values is the laser intensity.

At the end of the laser flash, however, a noticeable drop of the EEDF is observed when recombination losses are present, since in this case curve (I) (Ith=1.33x10^{11} w/cm^2) lies curve (II) (I_{th}=9x10^{10} w/cm^2) over the energy rang (1 to 11) eV. The coincidence of the two curves observed on the energy rang (11 to 19) eV, indicates the effect of recombination losses during the second half of laser pulse where electrons recombine with positive ions causing limitation of the growth of the electrons of energies higher than 12 eV.

Conclusions and Recommendations:

This research presents a general numerical modeling of electron cascade processes leading to breakdown in argon gas. The model succeed to interpret the breakdown phenomenon in argon gas over pressure range (1.368x10^2 torr to 2.35x10^3 torr) irradiated with the second harmonic of the Nd:galss laser of wave length is equal 0.53 μm and pulse duration is 15 ns. The EEDF gradually decreases up 12 eV (first excitation limit) followed by a sharp decrease resulting in a tail at ε = 21 eV ending with a very small value of the EEDF ~1 to 10. This gradual decrease can be explained due to the fast energy gain in elastic processes associated with the laser filed which causes an accumulation of energy to values exceeding the excitation (or ionization) threshold of the gas atoms, eventually causing their excitation or ionization. This result clarifies that during the first half of the laser flash losses has no contribution to the values of the EEDF. The only parameter which affect these values is the laser intensity. At the end of the laser flash, however, a noticeable drop of the EEDF is observed when recombination losses are present.

References:

1- P.S. Dalyander a, I.B. Gornushkin b, D.W. Hahn" Numerical simulation of laser-induced breakdown spectroscopy: Modeling of aerosol analysis with finite diffusion and vaporization effects" Spectrochimica Acta Part B 63 (2008) 293–304, United States.

2- C. V. Bindhu, S. S. Harilal,a) M. S. Tillack, F. Najmabadi, and A. C. Gaeris "Laser propagation and energy absorption by an argon spark" , J. Appl. Phys., Vol. 94, No. 12, 15 December 2003 7402- 7406.

3- Michał Lech * and PawełW˛egierek. Breakdown Initiation and Electrical Strength of a Vacuum
Insulating System in the Environment of Selected Noble Gases at AC Voltage, Energies 2022, 15, 1154.

4- B. Ghazolin, "Analytical studying of the effect of loss processes on Laser Induced Breakdown in Argon Gas ". Tishreen University Basic Science Series (2014) , Vol. 36 No. 2

5- Guy M. Weyle & David Rosen " Laser induced breakdown in argon at 0.35 □m: Theory and expermiment" Physical Review 1985 A Vol. 31 No. 4 , 2300-2313.

6- G.J.Fetzer. Rocca, and G. J. Collins. "Model od cw argon ion laser excited by low energy electron beams" J. Appl. Phys. 60(8), October 1986 . 2739-2753.

7- D.J. Rosen and G. Weyl. " Laser induced break down in nitrogen and rar gases at 0.53 and 0.35 □m " , J. Appl. Phys. 20(1987), 1264-1276.

8- C. V. Bindhu, S. S. Harilal,a) M. S. Tillack, F. Najmabadi, and A. C. Gaeris " Laser propagation and energy absorption by an argon spark " , , J. Appl. Phys., Vol. 94, No. 12, 15 December 2003, 7402-7407

9- Yoser E E-D Gamal," on Stepwise ionisation processes in electrical breakdown of molecular gases by laser radiation" J. Phys D: Appl. Phys. 22 (1989)385-389.

10- Shunsuke KASHIWAKURA† and Kazuaki WAGATSUMA. "Characteristics of the Calibration Curves of Copper for the Rapid Sorting of Steel Scrap by Means of Laser-induced Breakdown Spectroscopy under Ambient Air Atmospheres “. ANALYTICAL SCIENCES DECEMBER 2013, VOL. 29.